# Four-circle diffractometry for surfaces (invited)

I. K. Robinson

*AT&T Bell Laboratories, Murray Hill, New Jersey 07974*

(Presented on 1 September 1988)

Angle calculations for the four-circle diffractometer are usually made by the method of Busing and Levy [Acta Cryst. 22, 457 (1967)]. Here an additional mode of operation is described that allows control of the incident and exit angles at the sample surface. Experiences with this mode for surface crystallographic data collection are described.

## INTRODUCTION

Much progress has been made in recent years in the application of x-ray diffraction to surface structure and surface morphology problems. A major reason for its success is that, in the wavelength region used, the scattering is accurately kinematical, so that results may be interpreted by linear superposition techniques, including Fourier transformation. Another, less widely appreciated, advantage is that x-ray diffraction as a technique has a long history of instrumentation development and an associated manufacturing industry to provide reliable experimental apparatus. The Weisenberg, Laue rotation and precession methods are a few examples of data collection techniques developed over the years that are now highly advanced.[1] With the advent of more powerful sources and computer control, the four-circle diffractometer has gained a large clientele of users and is now the most widely used data collection method in x-ray diffraction. Its advantages (over film-based techniques) are its very large dynamic range, greater than $10^8$ between strongly and weakly scattering features, and its very high accuracy, routinely 1% in intensity and 0.001° in absolute angles.[2]

Angle calculations for the four-circle diffractometer are usually made by the method of Busing and Levy.[3] The definition of the four angles $2\theta$, $\theta$, $\chi$, and $\phi$ is given in Fig. 1. $2\theta$ is the angle of the detector to the incident beam. $2\theta$ is thus the diffraction angle dictated by Bragg's law

$$|\mathbf{Q}| = 2|\mathbf{k}| \sin(2\theta/2), \tag{1}$$

where $\mathbf{k}$ is the incident wave vector ($2\pi$/wavelength) and $\mathbf{Q}$ is the momentum transfer in the reciprocal lattice of the crystal. $\mathbf{Q}$ can be written in terms of Miller indices, $hk$ and $l$, multiplying the reciprocal lattice basis vectors $\mathbf{a}^*$, $\mathbf{b}^*$, and $\mathbf{c}^*$:

$$\mathbf{Q} = h\mathbf{a}^* + k\mathbf{b}^* + l\mathbf{c}^*. \tag{2}$$

$hk$ and $l$ are integers in a crystallographic problem, continuous variables in a diffuse scattering or line-shape analysis problem, or a combination of both in a surface problem which has a two-dimensional (2D) reciprocal lattice, and continuous symmetry in the direction perpendicular to the surface. Conventionally $\mathbf{a}^*$ and $\mathbf{b}^*$ are taken to be in-plane and $\mathbf{c}^*$ to be along the surface normal.[4] 2D plane group symmetry is assumed, but calculations are usually done in the analogous 3D monoclinic, orthorhombic, hexagonal, or tetragonal space groups with minimal symmetry operations in the $\mathbf{c}^*$ direction.

The sample is moved by the remaining three angles $\theta$, $\chi$, and $\phi$, which make an Eulerian triple. The diffractometer moves in the laboratory frame in which the incident beam is fixed, so the orientation of the sample in the frame of the momentum transfer (bisector of the incident and exit wave vectors) is defined by the angles $\{\omega, \chi, \phi\}$ where

$$\omega = \theta - 2\theta/2. \tag{3}$$

Note that "$2\theta$" and $\theta$ are independent variables representing different motions, following the customary nomenclature.[3] The diffractometer equations are used to derive $\{\omega, \chi, \phi\}$ for a given $\mathbf{Q}$ input taking account of external data in the form of two matrices:

(i) the orientation matrix, U. This is an orthogonal (rotation) matrix with three implicit degrees of freedom that map the crystal reference frame onto the "diffractometer" frame which can be considered to move on the $\phi$ table of the diffractometer:

$$\mathbf{h}_\phi = \mathsf{U}\mathbf{Q}. \tag{4}$$

(ii) the diffractometer rotation matrix, $\mathsf{R}(\omega,\chi,\phi)$. This represents the setting of the diffractometer and so maps the diffractometer frame onto the laboratory frame that bisects the incident and exit beams in Fig. 1.

Defining the $x$ direction to be parallel to the momentum transfer in the lab frame the basic diffractometer equation is written:

$$\begin{pmatrix}1\\0\\0\end{pmatrix} = \frac{1}{|\mathbf{Q}|}\mathsf{R}\mathsf{U}\mathbf{Q}. \tag{5}$$

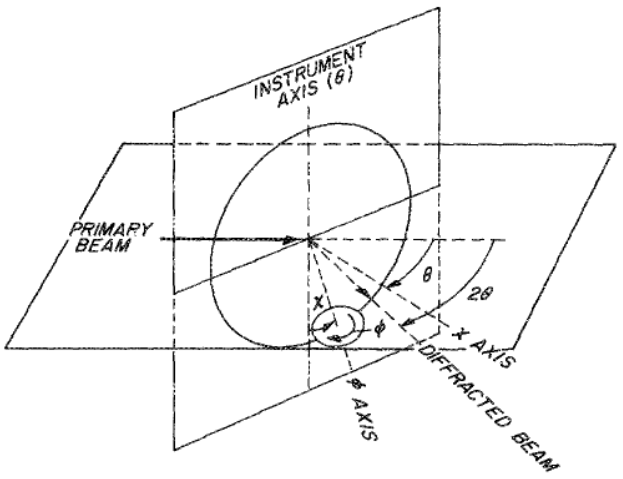


FIG. 1. The four-circle diffractometer and conventional definition of the angles.

 0034-6748/89/071541-04$01.30  

Busing and Levy show how to solve this equation for the angles and how the matrix U may be constructed from the positions of two standard reflections.[3]

Since Eq. (5) relates unit vectors that imply two degrees of freedom, there is, in general, a one-dimensional set of possible $\{\omega, \chi, \phi\}$ that can satisfy it. To obtain a unique solution, it is necessary to impose a *constraint*. Busing and Levy discuss several possibilities.[3] Often, in practice, the constraint is dictated by the sample environmental hardware or the shape of the crystal. A simple realization of this is to freeze one of the diffractometer angles to a constant value; the equation for doing this has been worked out by Braslau.[5] The simplest constraint of all is to set $\omega = 0$, as is very widely used on commercial diffractometers for crystallography and elsewhere.[2] It is then possible to visualize the solution in two steps. If $h_{\phi i}$ are the components of $\mathbf{h}_\phi$, then a rotation of $\phi = \arctan[h_{\phi 2}, h_{\phi 1}]$ brings the vector $\mathbf{h}_\phi$ into the bisecting plane which is the plane of the $\chi$ circle (see Fig. 1). Then to level this resulting vector to be along (1,0,0), a rotation of

$$\chi = \arctan[h_{\phi 3}, (h_{\phi 1}^2 + h_{\phi 2}^2)^{1/2}]$$

is needed.[3] Here we use the two-component arctangent, $\arctan[a,b]$, that is used in computer languages.

In the situation of surface x-ray diffraction we wish to make a new kind of constraint. This is an extreme limit of the sample shape problem because the sample is usually very wide and both the incident and exit beams must pass through the open face; the sample is, in effect, just one layer thick. Furthermore there are refraction effects in the diffracted intensity when either the incidence or exit angle is small.[6] While this can be avoided by working at a large angle, it is not always desirable because the thermal diffuse background is proportional to the penetration depth, which mounts rapidly when the incidence angle $\alpha$ is greater than the critical angle for total external reflection, $\alpha_c$. There are also some experiments that rely entirely on control of the incidence angle for surface sensitivity.[7] Other experiments just require control of the incidence and exit angles at the level of preventing them from becoming negative, which can happen if the sample alignment is not well understood.

The $\omega = 0$ mode works very well for surface diffraction provided the sample face is mounted exactly parallel to the $\phi$ table of the diffractometer, whereby the normal is along the $\phi$ axis. Then, there is a simple geometric relation between the diffractometer angles, the incidence angle $\alpha$, and the exit angle $\beta$ (Ref. 8):

$$\sin\alpha = \sin\beta = \sin\chi \sin\theta. \tag{6}$$

Furthermore, it is easy to show that $\sin\chi \sin\theta$ is proportional to $l$, the perpendicular component of momentum transfer (index conventions as defined above) since the orientation matrix U is just a rotation about $\phi$. Scans of intensity as a function of the continuous variable $l$ ("rod scans") are then scans of $\sin\alpha$, allowing the critical angle effects to be studied reliably. The symmetric relation of the two beams given by $\alpha = \beta$ allows the closest approach to $l = 0$ possible. It also simplifies the understanding of the resolution function and the consequential corrections to intensity measurements as functions of $l$.[9]

Unfortunately, it is not always possible to align the surface accurately, particularly in experiments involving ultrahigh vacuum hardware.[10] One solution is to construct an in-vacuum geometer to align the surface normal *in situ*, but this is not an easy accomplishment and prone to mechanical breakdowns.[11] Another solution, which is the subject of this paper, is to use the degree of freedom in Eq. (5) to set $\alpha = \beta$ for an arbitrary crystal orientation. It is important to keep a clear distinction between the *crystal* orientation (given by U) and the *surface* orientation (given by $\alpha = \beta$ in the formalism below). In general, a sample may not have a simple relation between these, and in fact, a number of interesting experiments may be conceived by varying one with respect to the other.[12]

## I. CALCULATION OF DIFFRACTOMETER ANGLES

Additional input must be provided to the calculation to define the direction of the surface. One way to do this is to specify its exact crystallographic direction which, given its orientation U, defines the physical direction. Experimentally this needs to be determined and optimized during the course of measurement, so we choose to make an operational definition: we define $\phi_0$ and $\chi_0$ to be the diffractometer angles that bring the surface normal onto the principal diffractometer axis ($\theta$ axis). In practice a laser would be set up to reflect from the surface; after adjustment of $\phi_0$ and $\chi_0$ until the surface is flat, the reflected beam does not move as the sample is rotated in $\theta$. These angles specify a unit vector $\hat{\mathbf{n}}_\phi$ which is the direction of the normal in the diffractometer frame (see above):

$$\hat{\mathbf{n}}_\phi = \begin{pmatrix} -\sin\chi_0 \cos\phi_0 \\ -\sin\chi_0 \sin\phi_0 \\ \cos\chi_0 \end{pmatrix}. \tag{7}$$

We can now set up the constraint equation to be solved simultaneously with Eq. (5). The desired crystal direction must be along (1,0,0) in the lab frame, but we have the freedom to rotate about that vector. We wish to place the surface normal $\hat{\mathbf{n}}_\phi$ into the $x$-$z$ plane in the lab frame (that bisects the incident and exit beams). This guarantees the symmetric beam arrangement on the sample with $\alpha = \beta$ shown in Fig. 2. Geometrically we therefore require $\mathbf{h}_\phi \wedge \hat{\mathbf{n}}_\phi$ to be along (0,1,0) and so can construct the entire R matrix from the mapping of three orthogonal unit vectors. Defining

$$\hat{\mathbf{h}}_\phi = (1/|\mathbf{Q}|)\mathsf{U}\mathbf{Q}. \tag{8}$$

Then

$$\begin{pmatrix} 1 \\ 0 \\ 0 \end{pmatrix} = \mathsf{R}\hat{\mathbf{h}}_\phi,$$

$$\begin{pmatrix} 0 \\ 1 \\ 0 \end{pmatrix} = \eta\mathsf{R}(\hat{\mathbf{h}}_\phi \wedge \hat{\mathbf{n}}_\phi),$$

$$\begin{pmatrix} 0 \\ 0 \\ 1 \end{pmatrix} = \eta\mathsf{R}[\hat{\mathbf{h}}_\phi \wedge (\hat{\mathbf{h}}_\phi \wedge \hat{\mathbf{n}}_\phi)], \tag{9}$$

where $\eta = 1/|\hat{\mathbf{h}}_\phi \wedge \hat{\mathbf{n}}_\phi|$ is a normalization constant. Hence

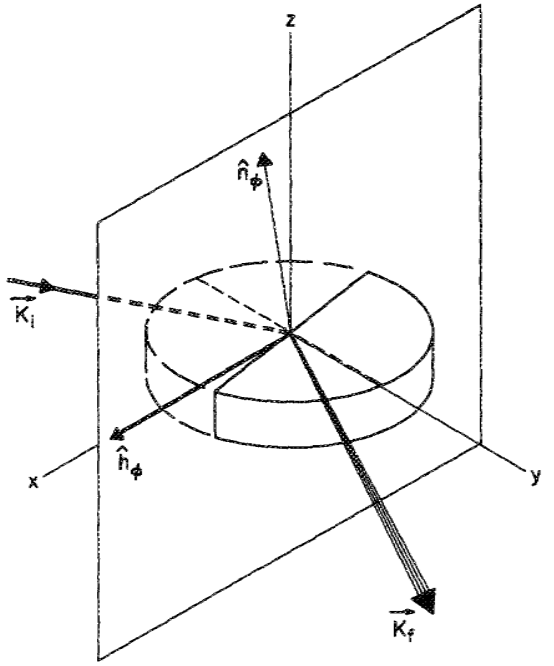


FIG. 2. Diffraction geometry for a surface. The sample is drawn as a solid disk. The direction of the reciprocal space point being measured, $\hat{h}_\phi$, and that of the surface normal, $\hat{n}_\phi$, are constrained to lie in the $x$-$z$ plane (in the lab frame) that bisects the incident and exit beams.

$$\mathsf{R} = [\hat{\mathbf{h}}_\phi; \eta\hat{\mathbf{h}}_\phi \wedge \hat{\mathbf{n}}_\phi; \eta\hat{\mathbf{h}}_\phi \wedge (\hat{\mathbf{h}}_\phi \wedge \hat{\mathbf{n}}_\phi)]^T. \quad (10)$$

From this we can compare terms with the definition of R in Euler angles $\{\omega, \chi, \phi\}$ to obtain explicit expressions for the angles themselves:

$$\omega = \arctan[m(a_2\hat{h}_{\phi 1} - a_1\hat{h}_{\phi 2}), |\hat{h}_{\phi 3}|],$$
$$\chi = \arctan[m(a_1^2 + a_2^2)^{1/2}, a_3],$$
$$\phi = \arctan[-ma_2, -ma_1], \quad (11)$$

where we have written our explicit components $\hat{h}_{\phi j}$ and $\hat{n}_{\phi j}$ of the unit vectors $\hat{\mathbf{h}}_\phi$ and $\hat{\mathbf{n}}_\phi$ defined in Eqs. (7) and (8) above, and made the following substitutions:

$$a_j = (\hat{n}_{\phi j} - s\hat{h}_{\phi j})/(1 - s^2)^{1/2},$$
$$s = \hat{n}_{\phi 1}\hat{h}_{\phi 1} + \hat{n}_{\phi 2}\hat{h}_{\phi 2} + \hat{n}_{\phi 3}\hat{h}_{\phi 3},$$
$$m = \text{sign}(\hat{h}_{\phi 3}).$$

Note that the range of angles has been constrained to $-90° < \omega < 90°$ and that other convections could have been used.

The diffractometer equation (11) degenerate to the result for $\omega = 0$ quoted above when $\chi_0 = 0$ in Eq. (7); this corresponds to the sample being mounted squarely on the $\phi$ axis which gives $\alpha = \beta$ as described. Otherwise a nonzero $\omega$ angle is obtained. When the tilt of the sample on the table is small, the equations provide a deviation in $\omega$ that compensates for the asymmetry between $\alpha$ and $\beta$ that would otherwise occur.

## II. APPLICATION

Our ultrahigh vacuum (UHV) diffractometer[10] is presently stationed at beamline X16A of the National Synchrotron Light Source (NSLS), Brookhaven. It is based on the four-circle convention but operates with a range of accessible $\chi$ angles of $\pm 12°$ limited by the UHV hardware; this, in effect, limits the range of accessible out-of-plane momentum transfer, $l$. We have performed experiments both in the $\omega = 0$ mode and the new mode, which we call "azimuth = 0." We compare the results here.

The first experiments were with Si(111) surfaces, which exhibit a $7\times7$ reconstruction when clean. The sample was mounted as close as possible to parallel to the $\phi$ axis. By use of the laser reflection technique we established $\chi_0 = 0.40°$, $\phi_0 = 32°$ for the true direction of the optical surface. After crystallographic alignment using bulk Bragg reflections the direction of the normal was calculated to be $(-0.003, -0.002, 1)$ in the hexagonal coordinate frame of the surface:

$$a^* = 0.2699\ \text{Å}^{-1}, \quad b^* = 0.2699\ \text{Å}^{-1},$$
$$c^* = 0.668\ \text{Å}^{-1}, \quad \gamma^* = 60°.$$

(see Ref. 13). Integrated intensities from surface Bragg reflections of the reconstruction were measured for four symmetry equivalents to determine their reproducibility. In the $\omega = 0$ mode, such data were collected for 120 different reflections with the error determined by the reproducibility of equivalents. It was found that reliable (12%) data could only be collected at $l \geqslant 0.15$; below that, the misorientation of the surface led to errors in intensity, either by losing the diffraction signal altogether, or by enhancement due to refraction. With such a large incidence angle, several times $\alpha_c$, a substantial background was measured under the data, reducing its accuracy upon integration. In the $\omega = 0$ mode without perfect alignment it is impossible to tame the refraction effects (for crystallographic work), because the same $\alpha$ and $\beta$ angles have to be maintained for all reflections. Without the azimuth = 0 mode, it is better to stay well *above* the critical angle and live with the background.

We studied the reproducibility of the (0,6,$l$) surface reflection with the azimuth = 0 mode giving the results shown in Table I. We used scans in $l$ to observe how the point of maximum intensity ($l_{max}$) varied with the choice of $\chi_0$ parameter input to the calculation through Eq. (7). The best reproducibility occurred at $\chi_0 = 0.4°$ in agreement with the experimental value found with the laser. When $\chi_0$ and $\phi_0$ are set correctly the value of the maximum is at $l = 0.035$ for all reflections; this corresponds to a perpendicular momentum transfer of 0.023 Å$^{-1}$ and by Eq. (6) to an incidence

TABLE I. Experimental values of $l_{max}$, the perpendicular component of momentum transfer that gives the maximum intensity, for two crystallographically equivalent reflections 60° apart. Such $l$ scans have no intensity for $l \ll l_{max}$, and a constant value for $l \gg l_{max}$; the maximum is due to refraction effects (Ref. 6).

| $\chi_0$ | 6,0,$l$ | 0,6,$l$ |
|---|---|---|
| 0.2 | 0.01 | 0.08 |
| 0.4 | 0.03 | 0.045 |
| 0.6 | 0.05 | 0.02 |
| 0.8 | 0.065 | <0 |

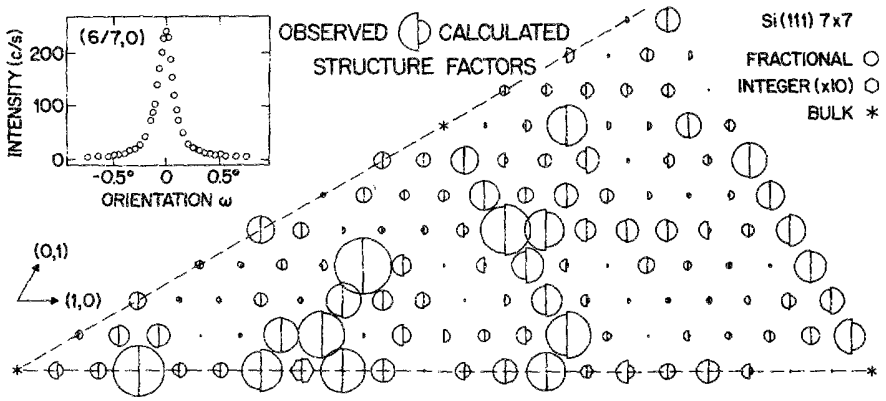


FIG. 3. Crystallographic data for the Si(111) 7×7 reconstructed surface, showing the agreement between calculation and observation. Inset is a typical rocking curve; the profile indicates an exponential correlation function with characteristic length 1500 Å. The coordinate frame is hexagonal and described in the text.

( = exit) angle of 0.123°, close to the value of $\alpha_c$ for Si with a wavelength of $\lambda = 1.157$ Å. A small set of data were then collected at $l = 0.035$ with comparable reproducibility to the large set and without any problems of lost reflections.

The analysis of the data has been published previously,[13] but is summarized here for completeness. A $\chi^2$ value of 1.6 (the value is 1.9 when the degrees of freedom are included in its definition[14]) between observed and calculated intensities is obtained and shown in Fig. 3. The model used to obtain this agreement is shown in Fig. 4 and is a refinement of the atomic positions proposed by Takayanagi *et al.*[15] for Si(111) 7×7. The same model applies to the 7×7 structure obtained by Sn absorption on Ge(111).[14]

Finally we note that the equations described have been incorporated into the "super" diffractometer control program in use at NSLS and elsewhere.[16] A different but related scheme for handling the orientation of surfaces in four-circle diffractometry has been described by Mochrie[17] and has been installed in the program "spec"[18] also in use at NSLS. Calculations for a five-circle diffractometer used to control incidence and exit angles independently have also been published.[19]

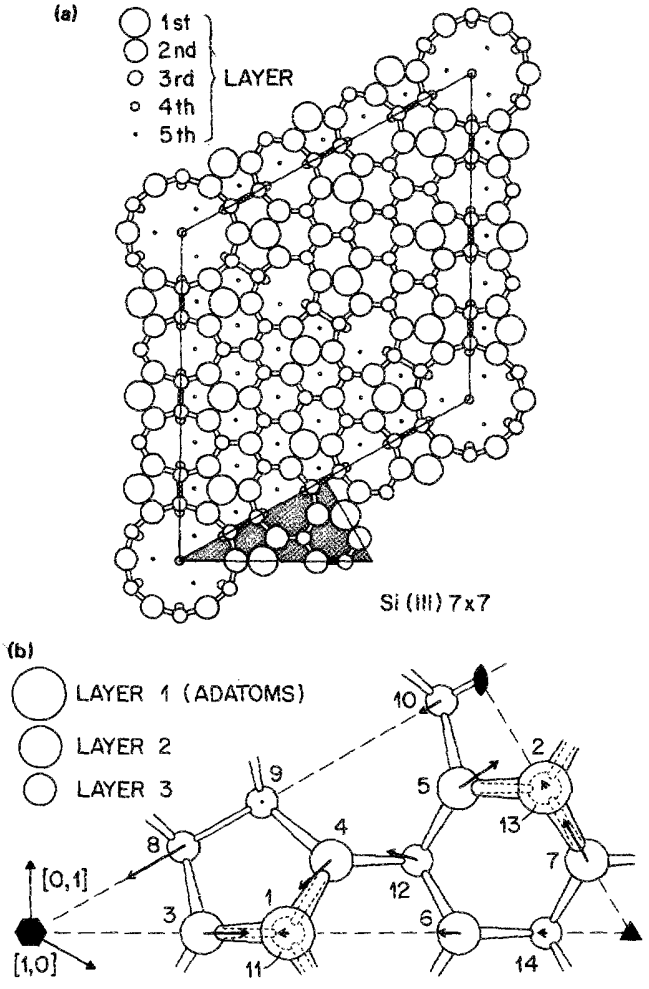


FIG. 4. (a) Atomic model of a unit cell of the Si(111) 7×7 surface due to Takayanagi *et al.* (Ref. 15). The shaded triangle is the crystallographic asymmetric unit. (b) Displacements of the atoms enlarged ten times within the asymmetric unit, as refined using the data of Fig. 3. The pattern of strain in the surface is evident.

## ACKNOWLEDGMENTS

Helpful discussions with S. G. J. Mochrie and R. M. Fleming are acknowledged. NSLS is supported by the U.S. DOE under Grant No. DE AC02 76 CH 00016.

[1] M. J. Buerger, in *X-ray Crystallography* (Wiley, New York, 1942).
[2] U. W. Arndt and B. T. M. Willis, in *Single Crystal Diffractometry* (Cambridge, London, 1966).
[3] W. R. Busing and H. A. Levy, Acta Cryst. **22**, 457 (1967).
[4] M. A. van Hove and S. Y. Tong, in *Surface Crystallography by LEED* (Springer, Berlin, 1978).
[5] A. Braslau, Ph.D. dissertation, Harvard Univ., 1987.
[6] M. Born and E. Wolf, in *Principles of Optics* (Pergamon, Oxford, 1959).
[7] H. Dosch, L. Mailänder, A. Lied, J. Peisl, F. Grey, R. L. Johnson, and S. Krummacher, Phys. Rev. Lett. **60**, 2382 (1988).
[8] I. K. Robinson, in *Handbook on Synchrotron Radiation*, Vol. 3, edited by D. E. Moncton and G. S. Brown (North Holland, Amsterdam, 1988).
[9] I. K. Robinson, Austral. J. Phys. **41**, 359 (1988).
[10] P. H. Fuoss and I. K. Robinson, Nucl. Instrum. Methods **222**, 171 (1984).
[11] P. Claverie, Thèse de docteur ingenieur Univ. de Clermont II, 1986.
[12] B. M. Ocko and S. G. J. Mochrie, Phys. Rev. B **38**, 7378 (1988).
[13] I. K. Robinson, W. K. Waskiewicz, P. H. Fuoss, and L. J. Norton, Phys. Rev. B **37**, 4325 (1988).
[14] J. S. Pedersen, Ph.D. dissertation, Univ. of Copenhagen, 1988.
[15] K. Takayanagi, Y. Tanishiro, S. Takahashi, and M. Takahashi, Surf. Sci. **164**, 367 (1985).
[16] R. M. Fleming (unpublished).
[17] S. G. J. Mochrie, J. Appl. Cryst. **21**, 1 (1988).
[18] G. Swislow, Certified Scientific Software, Cambridge, MA.
[19] E. Vlieg, J. F. van der Veen, J. E. Macdonald, and M. Miller, J. Appl. Cryst. **20**, 330 (1987).